*J. Fluid Mech.* (1982), *vol.* 121, *pp.* 43–58
*Printed in Great Britain*



# The propagation of two-dimensional and axisymmetric viscous gravity currents over a rigid horizontal surface

By HERBERT E. HUPPERT

Department of Applied Mathematics and Theoretical Physics, Silver Street, Cambridge CB3 9EW

(Received 2 September 1981 and in revised form 23 March 1982)

The viscous gravity current that results when fluid flows along a rigid horizontal surface below fluid of lesser density is analysed using a lubrication-theory approximation. It is shown that the effect on the gravity current of the motion in the upper fluid can be expressed as a condition of zero shear on the unknown upper surface of the gravity current. With the supposition that the volume of heavy fluid increases with time like $t^\alpha$, where $\alpha$ is a constant, a similarity solution to the governing nonlinear partial differential equations is obtained, which describes the shape and rate of propagation of the current. The viscous theory is shown to be valid for $t \gg t_1$ when $\alpha < \alpha_c$ and for $t \ll t_1$ when $\alpha > \alpha_c$, where $t_1$ is the transition time at which the inertial and viscous forces are equal, with $\alpha_c = \frac{1}{4}$ for a two-dimensional current and $\alpha_c = 3$ for an axisymmetric current. The solutions confirm the functional forms for the spreading relationships determined for $\alpha = 1$ in the preceding paper by Didden & Maxworthy (1982), as well as evaluating the multiplicative factors appearing in the relationships. The relationships compare very well with experimental measurements of the axisymmetric spreading of silicone oils into air for $\alpha = 0$ and 1. There is also very good agreement between the theoretical predictions and the measurements of the axisymmetric spreading of salt water into fresh water reported by Didden & Maxworthy and by Britter (1979). The predicted multiplicative constant is within 10% of that measured by Didden & Maxworthy for the spreading of salt water into fresh water in a channel.

## 1. Introduction

Open the front door of a centrally-heated house and a gravity current of cold air immediately flows in. The essential feature of such gravity currents is that fluid of one density flows primarily horizontally into fluid of a different density and the motion is driven by gravitational forces. Gravity currents originate in many different situations and have recently been subjected to extensive investigation. Interest in these flows spans the fields of geophysics, industrial engineering and geology, as is evident from the examples of thunderstorm outflows, polluted discharges into rivers or lakes, spreading lava domes and pyroclastic flows from volcanic explosions. Further examples are cited by Simpson (1982) in a recent review of the field.

Most investigators have studied high-Reynolds-number gravity currents, for which the motion is governed by a balance between buoyancy and inertial forces. In the preceding paper, Didden & Maxworthy (1982) consider low-Reynolds-number gravity currents propagating over a rigid horizontal surface, for which the motion is governed by a balance between buoyancy and viscous forces. Didden & Maxworthy

studied the rate of propagation of the front of two-dimensional and axisymmetric gravity currents due to a constant inflow rate of new fluid into fluid of much greater depth. From order-of-magnitude evaluations of the buoyancy forces, inertial forces and viscous forces, they obtained an estimate of the time, $t_1$ say, beyond which viscous forces overwhelm inertial forces. They also determined for $t \gg t_1$ dimensional relationships between the position of the front as a function of time and the external parameters. In a series of experiments they verified the functional forms of the position-versus-time relationships and evaluated the constants of proportionality from their experimental measurements.

Previous studies of low-Reynolds-number gravity currents include those by Fay (1969) and Hoult (1972), who analysed the release of a fixed volume of relatively light fluid flowing under a free surface. The viscous forces in this case are quite different to those relevant for the case of a relatively heavy current flowing along a rigid bottom. One can hence anticipate that the spreading relationships and shapes of the currents in the two cases will be entirely different. A pertinent result for viscous gravity currents propagating above a horizontal surface is briefly presented by Britter (1979). Britter performed a series of experiments using an axisymmetric geometry, in which a fixed flux of salt water was released into a very much deeper layer of fresh water. The experiments were designed mainly to investigate large-Reynolds-number gravity currents. However, in the last appendix of his paper, Britter reports data on the spreading relationships valid for times very much longer than the transition times $t_1$. We compare our theoretically determined results with these experimental ones in §4.

The primary aim of this paper is to determine entirely from theoretical considerations the spreading relationships for and shapes of two-dimensional and axisymmetric viscous gravity currents propagating over rigid horizontal surfaces. As sketched in figure 1, we consider fluid of density $\rho$ intruding into fluid of density $\rho - \Delta\rho$ ($\Delta\rho > 0$) and depth $H$ so that the volume at any time is proportional to $t^\alpha$, where $\alpha$ is some non-negative constant. Thus $\alpha = 0$ corresponds to the release of a constant volume of fluid and $\alpha = 1$ to a constant flux. In developing the theory we assume that the two fluids are not of greatly different viscosities and neglect the effects of mixing between them. We also neglect the effects of surface tension at the interface and at the front, or contact line. This requires that the Bond number $B = \rho g' a^2/T \gg 1$, where $g'$ is the reduced gravity, $a$ the length, or radius, of the current and $T$ the surface tension.

Only viscous and buoyancy effects are taken into consideration, so the theory can only be expected to be valid when the viscous forces are much larger than the inertial forces. This occurs when $\alpha < \alpha_c$ for $t \gg t_1$, where $t_1$ as a function of $\alpha$ and the other external parameters is estimated in appendix A, (equation (A7)) and $\alpha_c = \frac{7}{4}$ for a two-dimensional current and $\alpha_c = 3$ for an axisymmetric current. If $\alpha = \alpha_c$, the viscous forces greatly exceed the inertial forces, and do so for all time, provided that the Julian number $J = \nu^3 g'^2/q^4 \gg 1$ for two-dimensional currents or that $\nu g'/Q \gg 1$ for axisymmetric currents, where $q$ or $Q$ is the constant of proportionality between the volume of the current and $t^\alpha$. If the inequalities are reversed the current propagates under the influence of inertial forces. For $\alpha > \alpha_c$ the viscous forces initially dominate the inertial forces and so the viscous theory will be valid only for $t \ll t_1$; thereafter the influence of the inertial forces becomes important.

In all cases, except possibly at the initiation of the current, its length will greatly exceed its thickness, which allows for the boundary-layer approximation common to

lubrication theory to be used. We argue in §2, which presents the theoretical development, that the effect on the gravity current of the motion in the upper fluid can be entirely taken into account by applying the boundary condition of zero stress at the upper surface of the current. The current is thus identical with one propagating with a free surface beneath fluid of negligible inertia. The resulting nonlinear partial differential equations have similarity solutions which yield the shape and rate of propagation of the current.

For $\alpha = 1$, the only case considered by Didden & Maxworthy, the calculated functional forms of the position of the front of the current as a function of time are the same as evaluated by them. Further, our calculated value for the constant of proportionality is in excellent agreement with those presented for axisymmetric currents by Britter (1979) and by Didden & Maxworthy, but 10% higher than that presented by Didden & Maxworthy for two-dimensional currents. We discuss in more detail below a plausible explanation for this discrepancy which incorporates an estimate of the effects of drag at the sidewalls in the experiments.

Following the derivation and solution of the equations in §2, we present the results of a series of experiments with viscous silicone oils spreading axisymmetrically into air from either a fixed volume or fixed flux release. We find that there is extremely good agreement between our theoretically calculated and experimentally measured rate of spreading for both types of release. Accurate measurements of the thickness at the centre of the current for a fixed volume release are difficult to make, but the results of such measurements are shown to be in quite good agreement with the theory.

## 2. Theory

### 2.1. *Two-dimensional currents*

Consider a current of density $\rho$ intruding into a fluid of density $\rho - \Delta\rho$ and depth $H$. Since the vertical velocities are negligibly small, the pressure is hydrostatic and, with the co-ordinate system sketched in figure 1, the pressure in the gravity current is given by

$$p = p_0 + (\rho - \Delta\rho)\, g(H-h) + \rho g(h-z), \tag{2.1}$$

where $p_0$ is the (constant) pressure at $z = H$. The balance between the pressure gradient and the viscous forces is thus expressed by

$$\frac{1}{\rho}\frac{\partial p}{\partial x} = g'\frac{\partial h}{\partial x} = \nu\frac{\partial^2 u}{\partial z^2}, \tag{2.2}$$

where

$$g' = (\Delta\rho/\rho)\, g, \tag{2.3}$$

and horizontal derivatives have been neglected in comparison with vertical derivatives on the right-hand side of (2.2) because the length of the current is very much greater than its thickness. At the base of the current

$$u(x, 0, t) = 0, \tag{2.4}$$

and at the top of the current the shear stress is continuous and thus

$$\mu\frac{\partial u}{\partial z} = \mu_a\frac{\partial u_a}{\partial z} \quad (z = h), \tag{2.5}$$

where the subscript a refers to quantities in the ambient fluid. The motion in this

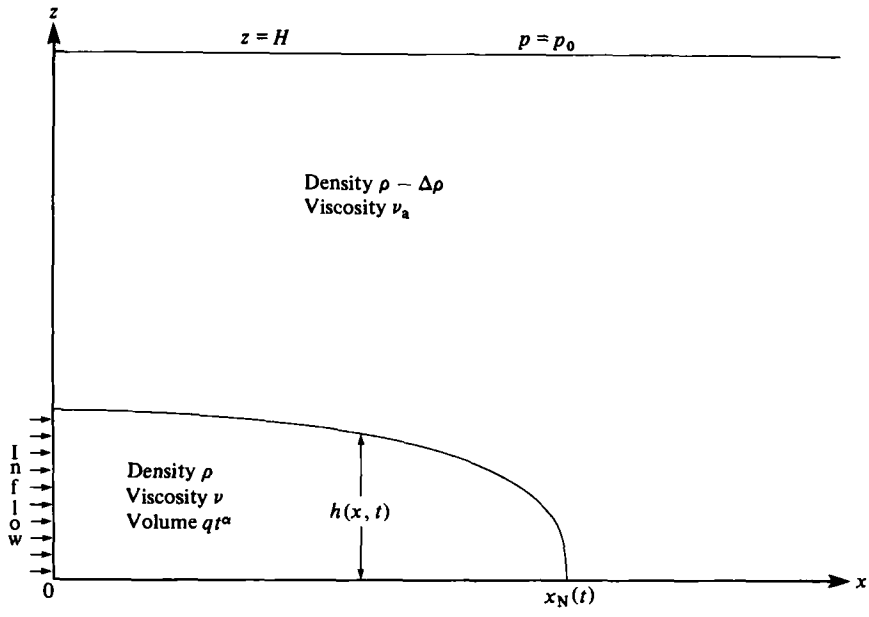


FIGURE 1. A sketch of the flow field and co-ordinate system.

fluid is due to viscous diffusion, and hence the ratio of the term on the right-hand side of (2.5) to that on the left is given, in order of magnitude, by $h_0/(\nu_a t)^{\frac{1}{2}}$, where $h_0$ is a representative thickness of the current. When the current is propagating under a buoyancy–viscous balance this ratio, as calculated in appendix B, is very much less than unity. The shear stress at the top of the current is hence very much less than its value within the current, and thus (2.5) can be approximated as

$$\frac{\partial u}{\partial z}(x, h, t) = 0. \tag{2.6}$$

The solution of (2.2), (2.4) and (2.6) is

$$u(x, z, t) = -\frac{1}{2}\frac{g'}{\nu}\frac{\partial h}{\partial x} z(2h - z). \tag{2.7}$$

Exactly the same velocity profile occurs if the motion in the ambient fluid is neglected, and at the top of the current the pressure is constant and the shear stress is zero. The flow is thus identical with that produced by a current spreading into fluid of negligible inertia. The physical explanation of this result is that the viscous dissipation in the current dominates over the dissipation in the fluid above it. A further relation between the unknowns $u$ and $h$ is

$$\frac{\partial h}{\partial t} + \frac{\partial}{\partial x}\left(\int_0^h u\, dz\right) = 0, \tag{2.8}$$

which is the depth-integrated version of the equation of continuity. Substituting (2.7) into (2.8), we obtain

$$\frac{\partial h}{\partial t} - \frac{1}{3}\frac{g'}{\nu}\frac{\partial}{\partial x}\left(h^3 \frac{\partial h}{\partial x}\right) = 0, \tag{2.9}$$

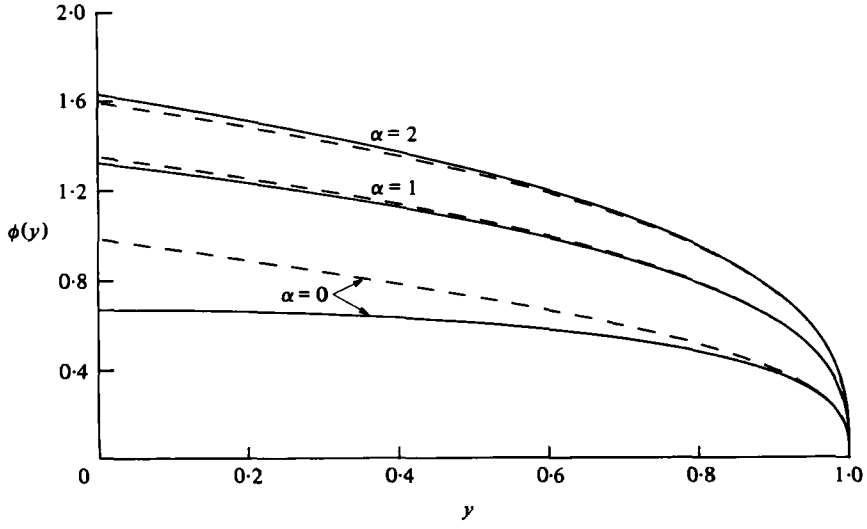


FIGURE 2. The shape of a two-dimensional viscous gravity current for $\alpha = 0$, 1 and 2. The dashed lines represent the approximate shapes (2.15).

as the governing nonlinear partial differential equation for $h(x, t)$. It is the global continuity equation

$$\int_0^{x_N(t)} h(x, t)\,dx = qt^\alpha \tag{2.10}$$

that completes the mathematical specification of the problem.

While numerical solutions to (2.9) and (2.10) for any given initial conditions could be obtained, it is much more fruitful to determine the similarity solutions of (2.9) and (2.10), to which all solutions with sufficiently regular initial conditions will tend except possibly at $x = 0$. The similarity solution can be expressed in terms of the similarity variable

$$\eta = (\tfrac{1}{3}g'q^3/\nu)^{-\frac{1}{5}}xt^{-(3\alpha+1)/5} \tag{2.11}$$

and the solution form

$$h(x, t) = \eta_N^{\frac{2}{3}}(3q^2\nu/g')^{\frac{1}{3}}t^{(2\alpha-1)/5}\phi(\eta/\eta_N), \tag{2.12}$$

where $\eta_N$ is the value of $\eta$ at $x = x_N(t)$. Substituting (2.11) and (2.12) into (2.9) and (2.10), we find that $\phi(y)$, where $y = \eta/\eta_N$, satisfies

$$(\phi^3\phi')' + \tfrac{1}{5}(3\alpha+1)\,y\phi' - \tfrac{1}{5}(2\alpha-1)\,\phi = 0, \tag{2.13}$$

and that

$$\eta_N = \left(\int_0^1 \phi\,dy\right)^{-\frac{3}{5}}. \tag{2.14}$$

Incorporating the condition that $\phi(1) = 0$ in (2.13), we find that about $y = 1$

$$\phi(y) = \left[\frac{3}{5}(3\alpha+1)\right]^{\frac{1}{3}}(1-y)^{\frac{1}{3}}\left[1 - \frac{3\alpha-4}{24(3\alpha+1)}(1-y) + O(1-y)^2\right], \tag{2.15}$$

which is sufficient to specify a unique solution of (2.13).

For arbitrary $\alpha$ the solution can only be obtained by numerically integrating (2.13) inward from $y = 1$ and using (2.15) as a starting condition. However, for $\alpha = 0$ the

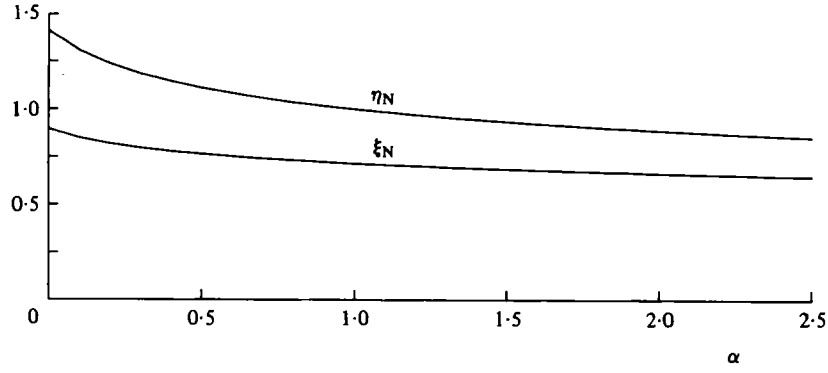


FIGURE 3. The values of the constants $\eta_N$ and $\xi_N$ as functions of $\alpha$.

solution of (2.13) and (2.14) can be obtained analytically, and is

$$\phi(y) = \left(\frac{3}{10}\right)^{\frac{1}{3}} (1-y^2)^{\frac{1}{3}}, \tag{2.16}$$

$$\eta_N = \left[\frac{1}{5}\left(\frac{3}{10}\right)^{\frac{1}{3}} \pi^{\frac{1}{2}}\Gamma(\tfrac{1}{3})/\Gamma(\tfrac{5}{6})\right]^{-\frac{3}{5}} = 1{\cdot}411\ldots, \tag{2.17}$$

as first determined by Pattle (1959). The existence of this analytic solution is convenient as it allows for a check to be made on the numerical integration schemes used to solve (2.13) and (2.14). Solutions of (2.13) for $\alpha = 0$, 1 and 2 are presented in figure 2, along with the first term in the expansion of the solution about $y = 1$ as given in (2.15). These approximate solutions are seen to agree quite well with the exact solutions. Note that, since at any fixed $x$ the mass flux is linearly proportional to the surface slope $\partial h/\partial x$, except for $\alpha = 0$ the slope of the exact solutions at $x = 0$ is non-zero, as is consistent with the fact that fluid is being continually introduced here. In figure 3 a graph of $\eta_N$ as a function of $\alpha$ is presented, from which the length of the current

$$L \equiv x_N(t) = \eta_N(\tfrac{1}{3}g'\, q^3/\nu)^{\frac{1}{5}} t^{(3\alpha+1)/5} \tag{2.18}$$

can be determined.

Note that there are no undetermined parameters in the solution, in contrast to the case of a relatively light current propagating under a free surface, analysed quantitatively by Hoult (1972). Hoult gives a clear description of the inadequacies of his approximations and an explanation of why he needed to resort to an experimental determination in order to complete the calculation. The important difference between the two studies is that in Hoult's case the motion of, and dissipation in, the ambient fluid determines the rate of propagation of the current. This is in contrast to our case, where the motion in the ambient fluid may be neglected.

### 2.2. *Axisymmetric currents*

The radial spreading of an axisymmetric current can be analysed in a similar manner to the spreading of a two-dimensional current. With a co-ordinate system as in figure 1 except that the radial co-ordinate $r$ replaces $x$, the velocity profile in the current is

$$u(r, z, t) = -\frac{1}{2}\frac{g'}{\nu}\frac{\partial h}{\partial r} z(2h-z). \tag{2.19}$$

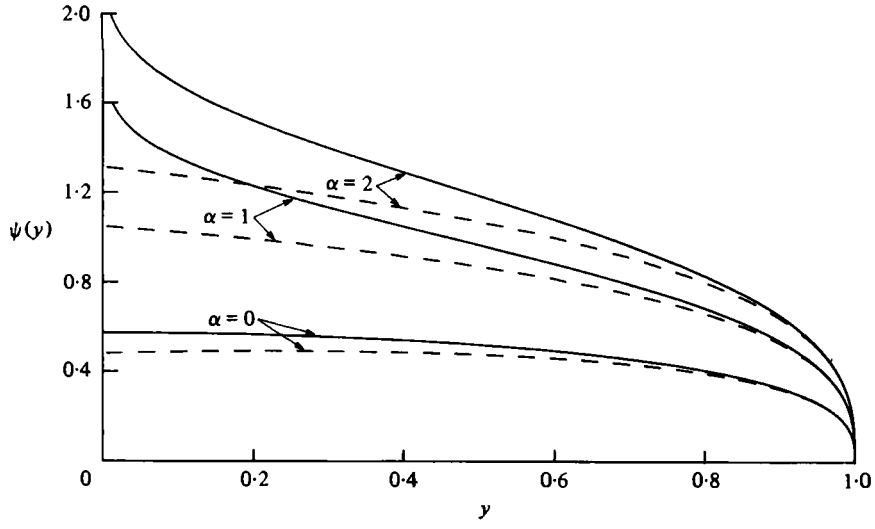


FIGURE 4. The shape of an axisymmetric viscous gravity current for $\alpha = 0$, 1 and 2. The dashed lines represent the approximate shapes (2.27).

The equation of continuity on a vertical sheet of radius $r$ is

$$\frac{\partial h}{\partial t}+\frac{1}{r}\frac{\partial}{\partial r}\left(r\int_0^h u\,dz\right)=0. \tag{2.20}$$

Substituting (2.19) into (2.20), we obtain

$$\frac{\partial h}{\partial t}-\frac{1}{3}\frac{g'}{\nu}\frac{1}{r}\frac{\partial}{\partial r}\left(rh^3\frac{\partial h}{\partial r}\right)=0, \tag{2.21}$$

to which must be added the global continuity equation

$$2\pi\int_0^{r_N(t)} rh(r,t)\,dr = Qt^\alpha. \tag{2.22}$$

A similarity solution of (2.21) and (2.22) can be obtained in terms of

$$\xi = (\tfrac{1}{3}g'Q^3/\nu)^{-\frac{1}{8}} rt^{-(3\alpha+1)/8} \tag{2.23}$$

and

$$h(r,t) = \xi_N^{\frac{3}{2}}(3Q\nu/g')^{\frac{1}{4}} t^{(\alpha-1)/4}\psi(\xi/\xi_N), \tag{2.24}$$

where $\xi_N$ is the value of $\xi$ at $r = r_N(t)$. Substituting (2.23) and (2.24) into (2.21) and (2.22), we find that $\psi(z)$, where $z = \xi/\xi_N$, satisfies

$$(z\psi^3\psi')'+\tfrac{1}{8}(3\alpha+1)z^2\psi'-\tfrac{1}{4}(\alpha-1)z\psi=0 \tag{2.25}$$

and that

$$\xi_N = \left[2\pi\int_0^1 z\psi(z)\,dz\right]^{-\frac{3}{8}}. \tag{2.26}$$

About $z = 1$, the solution is

$$\psi(z) = \left[\frac{3}{8}(3\alpha+1)\right]^{\frac{1}{3}}(1-z)^{\frac{1}{3}}\left[1-\frac{1}{3(3\alpha+1)}(1-z)+O(1-z)^2\right], \tag{2.27}$$

which is used as a starting condition in determining the numerical solution of (2.25).

(a)

| $Q$ (cm$^3$) | $\nu$ (cm$^2$ s$^{-1}$) | $c$ (0·894) | $p$ (0·125) | $k$ (1·0) | $q$ (−0·25) | |
|---|---|---|---|---|---|---|
| 387 | 13·2 | 0·873 ± 0·001 | 0·125 ± 0·002 | 0·916 ± 0·027 | −0·222 ± 0·009 | * |
| 933 | 13·2 | 0·860 ± 0·001 | 0·124 ± 0·005 | 1·314 ± 0·083 | −0·222 ± 0·036 | + |
| 406 | 13·2 | 0·900 ± 0·000 | 0·120 ± 0·002 | 0·704 ± 0·077 | −0·183 ± 0·025 | × |
| 338 | 1110 | 0·887 ± 0·000 | 0·122 ± 0·001 | 0·741 ± 0·008 | −0·196 ± 0·006 | □ |
| 220 | 13·2 | 0·877 ± 0·004 | 0·124 ± 0·002 | | | △ |

(b)

| $Q$ (cm$^3$ s$^{-1}$) | $\nu$ (cm$^2$ s$^{-1}$) | $K$ (0·715) | $r$ (0·5) | |
|---|---|---|---|---|
| 0·223 | 13·2 | 0·691 ± 0·010 | 0·501 ± 0·003 | × |
| 0·0493 | 13·2 | 0·692 ± 0·003 | 0·498 ± 0·001 | + |

TABLE 1. The parameters and results of all the experiments. In (*a*) $r_N = c(gQ^3/3\nu)^{\frac{1}{8}}t^p$, $h(0, t) = k(3\nu Q/4\pi g)^{\frac{1}{4}}t^q$; in (*b*) $r_N = K(gQ^3/3\nu)^{\frac{1}{8}}t^r$. The numbers in brackets in the column headings are the theoretical values of the parameters

For $\alpha = 0$ the following analytical solution can be obtained (Pattle, 1959):

$$\psi(z) = \left(\frac{3}{16}\right)^{\frac{1}{3}}(1-z^2)^{\frac{1}{3}}, \tag{2.28}$$

$$\xi_N = (2^{10}/3^4\pi^3)^{\frac{1}{8}} = 0{\cdot}894\ldots. \tag{2.29}$$

Solutions for $\alpha = 0$, 1 and 2 are presented in figure 4 along with the first term in the expansion about $z = 1$ as given in (2.27). Note that the exact solutions are singular at the origin unless $\alpha = 0$, reflecting the fact that fluid is being introduced at a non-zero rate at $r = 0$. Except in the vicinity of the origin the approximate solutions are seen to agree well with the exact ones. Figure 3 presents a graph of $\xi_N$ as a function of $\alpha$, and the radial extent of the current is given by

$$R \equiv r_N(t) = \xi_N(\tfrac{1}{3}g'Q^3/\nu)^{\frac{1}{8}}t^{(3\alpha+1)/8}. \tag{2.30}$$

## 3. Experiments

Before comparing our results with those of Britter (1979) and Didden & Maxworthy (1982), we present the results of some of our own experiments. We conducted a series of experiments using two silicone oils, with viscosities 13·2 and 1110 cm$^2$ s$^{-1}$. These values were determined by dropping a series of different size ball bearings in the oil contained in a measuring cylinder and recording the terminal velocities. This approach led to errors of less than 1 % in determining the coefficients of viscosity. The experiments were designed to examine a new theory for the spreading of volcanic lava domes by Huppert *et al.* (1982) and further details of the experiments and geological applications can be found in that paper. The oil spread axisymmetrically on a horizontal sheet of Perspex, beneath which there was a mm ruled sheet of graph paper, which allowed the radius of the current as a function of time to be monitored.

Five experiments with a fixed volume release ($\alpha = 0$) were conducted. In the first two, at the start of each experiment the oil was poured near to the central point of the Perspex. In the next two, the oil was initially held in a cylinder of radius 4·5 cm, which was raised at the start of the experiment. In the last experiment the oil was initially confined in a Perspex cylinder with internal dimension of $h = \frac{1}{7}(7-r)^2$. The value of $Q$, documented for each experiment in table 1, represents the total amount

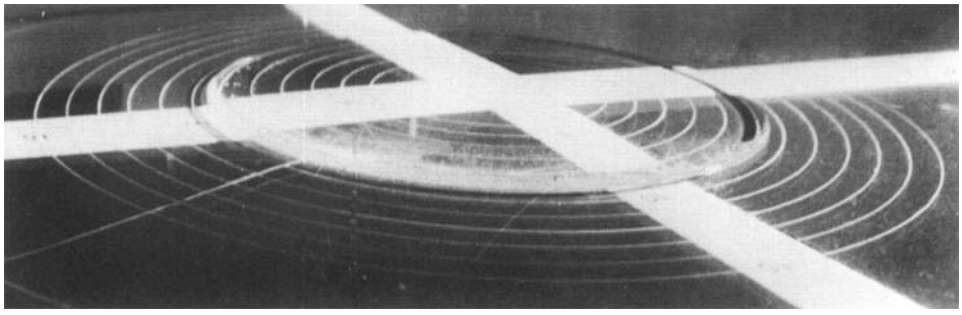

FIGURE 5. A laboratory gravity current due to 400 cm$^3$ of silicone oil with $\nu = 13{\cdot}2$ cm$^2$ s$^{-1}$, spreading axisymmetrically into air approximately 12 min after release.

of oil released, after allowing, if necessary, for any oil remaining on the sides of the releasing cylinders. As will be seen from the data, the mode of initiation made no difference after a few seconds from release. The height of the oil at the central point was measured by lowering a micrometer onto the surface, though it was difficult to judge when the micrometer top was just on the surface. Additionally, there frequently appeared to be some electrostatic attraction between the micrometer tip and the surface of the oil which resulted in a series of stationary concentric ripples.

Table 1 lists the conditions of each experiment and the best-fit parameters for the results, as defined in the caption. A photograph of a typical current is reproduced in figure 5. Figure 6 presents the results of all five experiments. With the radial extent of the current normalized by $(gQ^3/3\nu)^{\frac{1}{8}}$, as suggested by (2.30), the data are seen to fall together on a universal curve. The best-fit power law through the data is

$$r_N = (0{\cdot}887 \pm 0{\cdot}002)\,(gQ^3/3\nu)^{\frac{1}{8}}\,t^{0{\cdot}122 \pm 0{\cdot}002} \tag{3.1}$$

which is in good agreement with the theoretical relationship

$$r_N = 0{\cdot}894\ (gQ^3/3\nu)^{\frac{1}{8}}\,t^{0{\cdot}125}. \tag{3.2}$$

The data on the height of the current at the centre is more scattered – owing to the difficulty of making the measurements – though when normalized by $(3\nu Q/4\pi g)^{\frac{1}{4}}$, as suggested by (2.24), (2.28) and (2.29) they fall together reasonably well. The best-fit power law through the data is

$$h(0, t) = (0{\cdot}94 \pm 0{\cdot}04)\,(3\nu Q/4\pi g)^{\frac{1}{4}}\,t^{-0{\cdot}22 \pm 0{\cdot}01}, \tag{3.3}$$

in reasonable agreement with the theoretical relationship

$$h(0, t) = (3\nu Q/4\pi g)^{\frac{1}{4}}\,t^{-0{\cdot}25}. \tag{3.4}$$

Two experiments with a constant flux release ($\alpha = 1$) were conducted. In the first the oil was released from a burette holding approximately 600 cm$^3$ maintained at a constant head and in the second from an LKB 12000 VarioPerspex pump. The conditions of both experiments and the best-fit parameters for the results are listed in table 1. Figure 7 presents a plot of the data. The best-fit power law is

$$r_N = (0{\cdot}694 \pm 0{\cdot}004)\,(gQ^3/3\nu)^{\frac{1}{8}}\,t^{0{\cdot}499 \pm 0{\cdot}001}, \tag{3·5}$$

to be compared with the theoretical relationship

$$r_N = 0{\cdot}715(gQ^3/3\nu)^{\frac{1}{8}}\,t^{0{\cdot}5}. \tag{3.6}$$

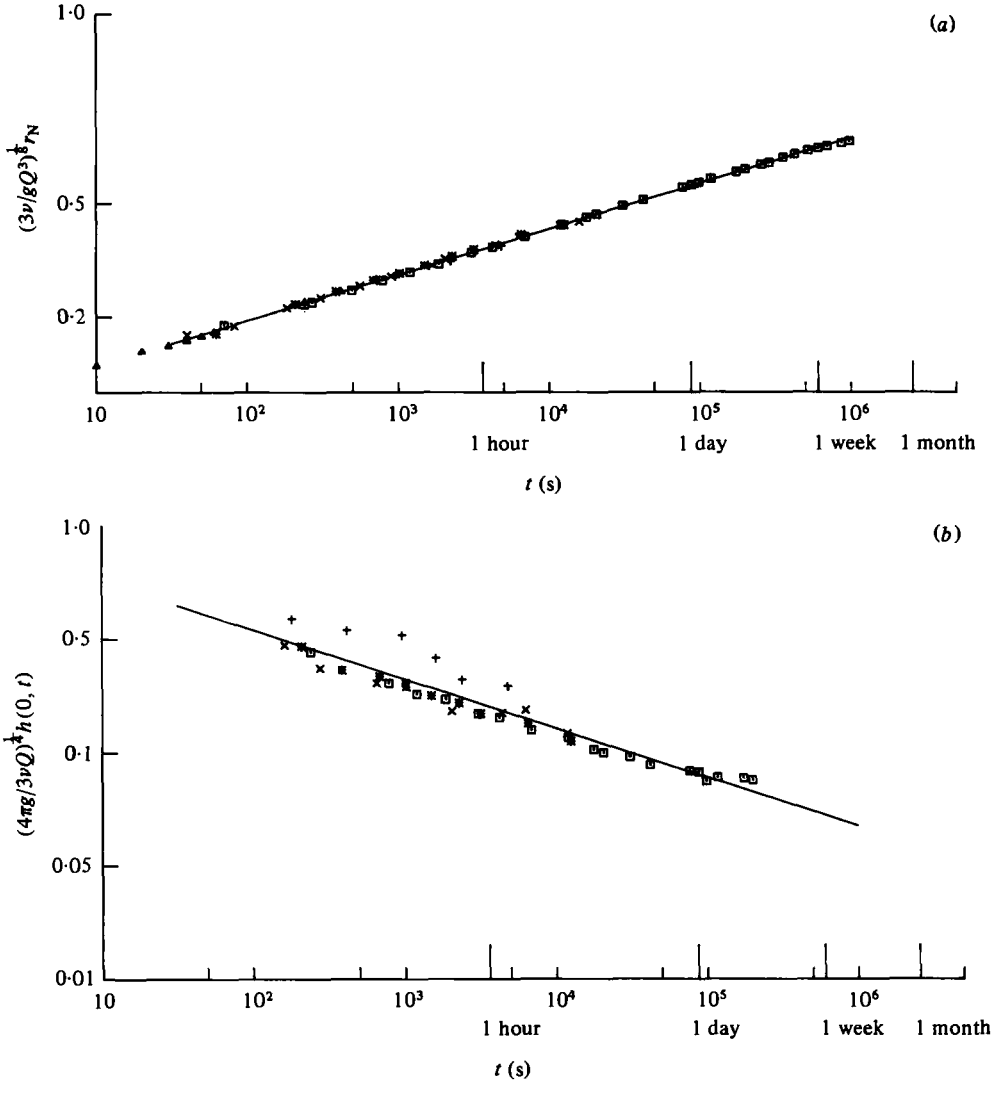


FIGURE 6. (*a*) Experimental values of $(3\nu/gQ^3)^{\frac{1}{3}}r_N$ as a function of time for the axisymmetric spreading of constant volumes of silicone oils into air. The straight line is the best-fit power law (3·1). (*b*) Experimental values of $(4\pi g/3\nu Q)^{\frac{1}{4}}h(0,t)$ as a function of time for the axisymmetric spreading of constant volumes of silicone oils into air. The straight line is the best-fit power law (3.3).

## 4. Discussion

Section 3 described the close agreement between our theoretical and experimental results for the axisymmetric spreading of oil into air. The comparison between our theoretical results and the experimental ones presented by Didden & Maxworthy (1982) for the axisymmetric spreading of salt water into fresh water is also very good. The theoretical spreading relationship, (2.30), predicts that

$$r_N = 0{\cdot}623\,(g'Q^3/\nu)^{\frac{1}{8}}t^{\frac{1}{2}}. \tag{4.1}$$

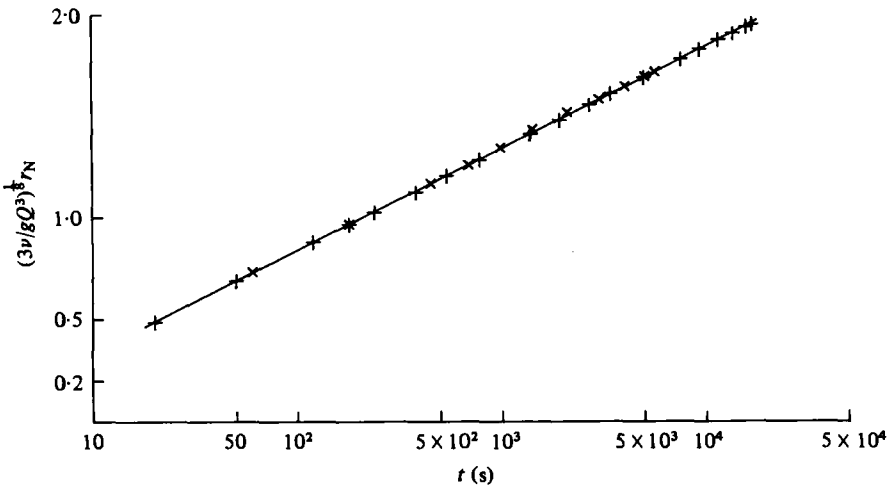


FIGURE 7. Experimental values of $(3\nu/gQ^3)^{\frac{1}{3}} r_N$ as a function of time for the axisymmetric spreading of silicone oils into air at constant efflux rates. The straight line is the best-fit power law (3.5).

This functional form is mirrored in the experimental measurements and the multiplicative constant is close to the measured value of $0{\cdot}60 \pm 0{\cdot}02$.

The comparison between the theoretical and experimental results for the spreading of salt water into fresh water in a wide channel is only fair. The theoretical prediction for entirely two-dimensional spreading is that

$$x_N = 0{\cdot}804\,(g'q^3/\nu)^{\frac{1}{5}} t^{\frac{4}{5}}. \tag{4.2}$$

This functional form is mirrored in the experimental results, but the multiplicative constant differs somewhat from the measured value of $0{\cdot}73 \pm 0{\cdot}03$. Given the close agreement in the previously cited experiments, the disagreement in this case must be due to an effect not present in the axisymmetric situation. The additional drag at the sidewalls of the experiment seems the only possible effect. Its relative importance will depend on the ratio, say $\lambda$, of channel width to current height. Didden & Maxworthy estimate the sidewall effects to reduce the multiplicative constant by up to 7 % – almost sufficient to bring the experimental results in agreement with the theoretical predictions – but no systematic variation in the multiplicative constant was found with $\lambda$.

The similarity between our theoretically determined relationship (4.1) and

$$r_N = (0{\cdot}67 \pm 0{\cdot}07)\,(g'Q^3/\nu)^{\frac{1}{5}} t^{\frac{2}{3}} \tag{4.3}$$

determined experimentally by Britter (1979) is particularly pleasing. Britter chose some of the values of $g'$ and $Q$ for his experiments of salt water propagating axisymmetrically into fresh water so that the transition times were as long as feasible. It thus appears from his data that even though a gravity current propagates through a lengthy buoyancy–inertial phase, once viscous effects become important after approximately $0{\cdot}4t_1$ the radius–time relationship quickly approaches that given by a buoyancy–viscous balance.

From a theoretical viewpoint, one of the most surprising results of this paper is that conditions at the front of the current play no role in determining its motion or shape. Indeed, the lubrication-theory profiles (2.7) and (2.19), which represent

| | Two-dimensional ($\alpha_c = \frac{7}{4}$) | | | Axisymmetric ($\alpha_c = 3$) | |
|---|---|---|---|---|---|
| | Buoyancy–inertial balance | Buoyancy–viscous balance | | Bouyancy–inertial balance | Buoyancy–viscous balance |
| | $L \sim (g'q)^{\frac{1}{3}} t^{(\alpha+2)/3}$ | $L \sim (g'q^3/\nu)^{\frac{1}{5}} t^{(3\alpha+1)/5}$ | | $R \sim (g'Q)^{\frac{1}{4}} t^{(\alpha+2)/4}$ | $R \sim (g'Q^3/\nu)^{\frac{1}{8}} t^{(3\alpha+1)/8}$ |
| $F_i/(\rho w) \sim qLt^{\alpha-2}$ | $(g'q^4)^{\frac{1}{3}} t^{4(\alpha-1)/3}$ | $(g'q^8/\nu)^{\frac{1}{5}} t^{(8\alpha-9)/5}$ | $F_l/\rho \sim QRt^{\alpha-2}$ | $(g'Q^5)^{\frac{1}{4}} t^{(5\alpha-6)/4}$ | $(g'Q^{11}/\nu)^{\frac{1}{8}} t^{(11\alpha-15)/8}$ |
| $F_v/(\rho w) \sim \nu q^{-1} L^3 t^{-\alpha-1}$ | $\nu g' t$ | $(g'^3 q^4 \nu^2)^{\frac{1}{5}} t^{2(2\alpha-1)/5}$ | $F_v/\rho \sim \nu Q^{-1} R^5 t^{-\alpha-1}$ | $\nu(g'^5 Q)^{\frac{1}{4}} t^{(\alpha+6)/4}$ | $\mu(g'^5 Q^7/\nu^5)^{\frac{1}{8}} t^{(7\alpha-3)/8}$ |
| $F_l/F_v$ | $(q^4 g'^2 \nu^3)^{\frac{1}{3}} t^{4(\alpha-\alpha_c)/3}$ | $(q^4/g'^2\nu^3)^{\frac{1}{5}} t^{4(\alpha-\alpha_c)/5}$ | $F_l/F_v$ | $(Q/g'\nu)\, t^{\alpha-\alpha_c}$ | $(Q/g'\nu)^{\frac{1}{2}} t^{(\alpha-\alpha_c)/2}$ |

TABLE 2. The formal values of the orders of magnitude of the inertial and viscous forces, and their ratios, for either two-dimensional or axisymmetric gravity currents propagating under either a buoyancy–inertia or a buoyancy–viscous balance. The forces are evaluated by the procedures discussed in appendix A

parallel flow, are totally incorrect at the front. Yet, by using them, solutions to the governing equations can be obtained without invoking any further conditions at the front. (The relationships (2.15) and (2.27), used to commence the integration of the differential equations, are obtained from them and are not an externally imposed condition.)

This lack of influence of the front will be true only if the Reynolds number is low and the Bond number is high. High-Reynolds-number gravity currents are totally controlled by conditions at the front, and many theoretical and experimental studies have been devoted almost entirely to determining the controlling condition, or Froude number, at the front (see, e.g. Benjamin 1968; Britter & Simpson 1978; Huppert & Simpson 1980). The front of a surface-tension-dominated (low-Bond-number) gravity current also plays an essential role in determining its spreading rate, as documented for example by Greenspan (1978) and Hocking (1981).

However, while our approach has been successful in predicting the overall shape – as evidenced by the experimental measurements of height presented in §3 – it should not be thought that the vertical front common to all the solutions is realistic. Contact-line effects will play a role in determining the exact shape at the front and the experiments showed clearly the curling over at the front, as evident in figure 5.

Another somewhat surprising result is the singularity at $\alpha = \alpha_c$ and the changeover in behaviour at this point. The evolution for $\alpha < \alpha_c$ from a buoyancy–inertial balance to a buoyancy–viscous balance is in accord with previous experience. As indicated by the expressions for the inertial and viscous forces and their ratio presented in table 2, for $\alpha < \alpha_c$ the viscous forces increase monotonically with time until they exceed the inertial forces (which may have been either increasing or decreasing monotonically with time) at $t = t_1$. Expressed in an alternative way, the ratio of inertial to viscous forces for $\alpha < \alpha_c$ is a monotonically *decreasing* function of time.

When $\alpha > \alpha_c$ the rate at which fluid is introduced is initially sufficiently small that inertial forces are comparatively low and viscous forces dominate. With increasing time, the volume flux increases and the inertial forces increase monotonically at a more rapid rate than the viscous forces (which also increase monotonically) so that beyond $t_1$ the inertial forces dominate. Alternatively, the ratio of inertial to viscous forces for $\alpha > \alpha_c$ is a monotonically *increasing* function of time.

For $\alpha = \alpha_c$ both inertial and viscous forces increase with time at the same rate. Thus the gravity current propagates under the same balance of forces for all time, and there is no transition region. It would be fun to conduct some experiments around and beyond $\alpha = \alpha_c$ to confirm (or possibly invalidate) the predictions in this regime.

It is a pleasure to thank Tony Maxworthy and Steve Sparks for a number of stimulating conversations, Rex Britter and Jim Rottman for very helpful readings of an earlier version of the paper, and Joyce Wheeler for assistance with performing the experiments, analysing the data and preparing the figures for publication. The research was supported by a grant from the Natural Environment Research Council.

*Notes added in proof.* (i) I am grateful to Professor G. I. Barenblatt, who has drawn my attention to the fact that the similarity solutions obtained for (2.9), (2.10) and (2.21), (2.22) can be derived from similarity solutions he discussed in Прикладная Математика и Механика vol. 16, 1952, pp. 67–78 and pp. 679–698. (ii) The pleasure in carrying out the experiments suggested in the last sentence of §4 has already been enjoyed by Tony Maxworthy, who finds that the predictions of the paper concerning

the form of motion about $\alpha = \alpha_c$ to be substantiated. In particular, his two-dimensional experiments indicate that there is a transition at $\alpha_c = \frac{7}{4}$ with a transition Julian number at $\alpha_c$ of approximately 7. The work is currently being considered for publication by this Journal.

## Appendix A

Using the arguments put forward by Didden & Maxworthy (1982), we determine in this appendix relationships for the transition time $t_1$ when inertia forces and viscous forces are comparable.

The prescribed input into the current requires that

$$h_0 L \sim qt^\alpha \quad \text{for two-dimensional spreading,} \tag{A 1a}$$

$$h_0 R^2 \sim Qt^\alpha \quad \text{for axisymmetric spreading,} \tag{A 1b}$$

where $h_0$ is a representative thickness of the current of length $L = x_N(t)$ or radius $R = r_N(t)$ and $\sim$ implies an order-of-magnitude relationship. The total buoyancy force is given by

$$F_g \sim \rho g' h_0^2 w \sim (\rho g' q^2 w/L^2)\, t^{2\alpha} \quad \text{for two-dimensional spreading} \tag{A 2a}$$

$$\sim \rho g' h_0^2 R \sim (\rho g' Q^2/R^3)\, t^{2\alpha} \quad \text{for axisymmetric spreading,} \tag{A 2b}$$

where $w$ is the width of the two-dimensional current. The inertial force is given by

$$F_i \sim \rho U^2 h_0 w \sim \rho q L w t^{\alpha-2} \quad \text{for two-dimensional spreading} \tag{A 3a}$$

$$\sim \rho U^2 h_0 R \sim \rho Q R t^{\alpha-2} \quad \text{for axisymmetric spreading,} \tag{A 3b}$$

where $U \sim L/t$ or $R/t$ is a representative velocity of the current. The viscous drag along the bottom of the current is given by

$$F_v \sim \mu U L w/h_0 \sim \mu q^{-1} L^3 w t^{-\alpha-1} \quad \text{for two-dimensional spreading} \tag{A 4a}$$

$$\sim \mu U R^2/h_0 \sim \mu Q^{-1} R^5 t^{-\alpha-1} \quad \text{for axisymmetric spreading.} \tag{A 4b}$$

Equating (A 2) and (A 3), we find that when the current propagates under a buoyancy–inertial balance

$$L \sim (g'q)^{\frac{1}{3}} t^{(\alpha+2)/3} \quad \text{for two-dimensional spreading,} \tag{A 5a}$$

$$R \sim (g'Q)^{\frac{1}{4}} t^{(\alpha+2)/4} \quad \text{for axisymmetric spreading.} \tag{A 5b}$$

When propagating under a buoyancy–viscous balance, as described by either (2.18) or (2.30), the ratio of the inertial forces to the viscous forces is given by

$$F_i/F_v \sim (q^4/g'^2\nu^3)^{\frac{1}{5}} t^{(4\alpha-7)/5} \quad \text{for two-dimensional spreading} \tag{A 6a}$$

$$\sim (Q/g'\nu)^{\frac{1}{2}} t^{(\alpha-3)/2} \quad \text{for axisymmetric spreading.} \tag{A 6b}$$

Thus the transition time at which inertial and viscous forces are comparable is given by

$$t_1 \sim (q^4/g'^2\nu^3)^{1/(7-4\alpha)} \quad \text{for two-dimensional spreading} \tag{A 7a}$$

$$\sim (Q/g'\nu)\, t^{1/(3-\alpha)} \quad \text{for axisymmetric spreading.} \tag{A 7b}$$

The same expression for $t_1$ results from equating (A 3) and (A 4) and using (A 5) rather than (2.18) or (2.30).

Expressions for the various forces are summarized in table 2, which presents formal

relationships for the inertial forces, given by (A 3), and the viscous forces, given by (A 4), when the extent of the current is given by either (A 5), (2.18) or (2.30).

The singularity at $\alpha = \alpha_c$ ($\alpha_c = \frac{7}{4}$ for two-dimensional spreading and $\alpha_c = 3$ for axisymmetric spreading) commented upon previously separates two distinct regimes. For $\alpha < \alpha_c$ the inertial forces are negligibly small compared with the viscous forces for $t \gg t_1$, and $t_1$ increases with increasing flow rate and decreases with increasing viscosity, as might be expected. For $\alpha = \alpha_c$ the inertial effects are insignificant for all time provided that either $J = \nu^3 g'^2/q^4 \gg 1$ or $\nu g'/Q \gg 1$. For $\alpha > \alpha_c$ the inertial forces may be neglected only if $t \ll t_1$, where $t_1$ decreases with increasing flow rate and increases with increasing velocity.

## Appendix B

In this appendix we prove that the continuity of velocity $u$ and shear stress $\mu \partial u/\partial x$ at the upper surface of the gravity current implies that the appropriate boundary condition there when the current propagates under a buoyancy–viscous balance is $\partial u/\partial z = 0$.

The lengthscale of the velocity profile in the gravity current is its thickness $h_0$, while that in the ambient fluid is the viscous-diffusion scale $(\nu_a t)^{\frac{1}{2}}$. Thus the ratio, say $S$, of the shear stress in the ambient fluid to that in the current is given by

$$S \sim h_0/(\nu t)^{\frac{1}{2}}, \tag{B 1}$$

supposing that the two fluids have not greatly differing viscosities. Using (2.18), (2.30), (A 1) and (A 6) we can express this ratio as

$$S \sim L^{-1} q t^{\alpha}/(\nu t)^{\frac{1}{2}} \sim (t/t_1)^{(4\alpha-7)/10} \quad \text{for two-dimensional spreading} \tag{B 2a}$$

$$\sim R^{-2} Q t^{\alpha}/(\nu t)^{\frac{1}{2}} \sim (t/t_1)^{(\alpha-3)/4} \quad \text{for axisymmetric spreading.} \tag{B 2b}$$

In both geometries, either for $\alpha < \alpha_c$ and $t \gg t_1$ or for $\alpha > \alpha_c$ and $t \ll t_1$, $S \ll 1$, and thus the shear at the top of the gravity current is effectively zero. For $\alpha = \alpha_c$

$$S \sim (g'^2 \nu^3/q^4)^{\frac{1}{10}} \quad \text{for two-dimensional spreading} \tag{B 3a}$$

$$\sim (g' \nu/Q)^{\frac{1}{2}} \quad \text{for axisymmetric spreading.} \tag{B 3b}$$

Again, in both geometries, under the conditions for the viscous forces to dominate the inertial forces, as given in the last paragraph of appendix A, $S \ll 1$ and the shear at the top of the gravity current may be set equal to zero.

## REFERENCES


BENJAMIN, T. B. 1968 Gravity currents and related phenomena. *J. Fluid Mech.* **31**, 209–248.

BRITTER, R. E. 1979 The spread of a negatively buoyant plume in a calm environment. *Atmos. Environ.* **13**, 1241–1247.

BRITTER, R. E. & SIMPSON, J. E. 1978 Experiments on the dynamics of a gravity current head. *J. Fluid Mech.* **88**, 223–240.

DIDDEN, N. & MAXWORTHY, T. 1982 The viscous spreading of plane and axisymmetric gravity currents. *J. Fluid Mech.* **121**, 27–42.

FAY, J. A. 1969 The spread of oil slicks on a calm sea. In *Oil on the Sea* (ed. D. P. Hoult), pp. 33–63. Plenum.

GREENSPAN, H. P. 1978 On the motion of a small viscous droplet that wets a surface. *J. Fluid Mech.* **84**, 125–143.

HOCKING, L. M. 1981 Sliding and spreading of thin two-dimensional drops. *Q. J. Mech. Appl. Math.* **34**, 37–55.

HOULT, D. P. 1972 Oil spreading on the sea. *Ann. Rev. Fluid Mech.* **4**, 341–368.

HUPPERT, H. E., SHEPHERD, J. B., SIGURDSSON, H. & SPARKS, R. S. J. 1982 On lava dome growth, with application to the 1979 lava extrusion of the Soufrière of St. Vincent. *J. Volcanol. Geotherm. Res.* **13** (in the press).

HUPPERT, H. E. & SIMPSON, J. E. 1980 The slumping of gravity currents. *J. Fluid Mech.* **99**, 785–799.

PATTLE, R. E. 1959 Diffusion from an instantaneous point source with a concentration-dependent coefficient. *Q. J. Mech. Appl. Math.* **12**, 407–409.

SIMPSON, J. E. 1982 Gravity currents in the laboratory, atmosphere, and ocean. *Ann. Rev. Fluid Mech.* **14**, 213–234.